JOC The Journal of Organic Chemistry

Article

pubs.acs.org/joc

Reactivity Indices Profile: A Companion Tool of the Potential Energy Surface for the Analysis of Reaction Mechanisms. Nucleophilic Aromatic Substitution Reactions as Test Case

Rodrigo Ormazábal-Toledo,*[,†] Renato Contreras,[†] and Paola R. Campodónico[‡]

[†]Departamento de Química, Facultad de Ciencias, Universidad de Chile, Casilla 653, Santiago, Chile

[‡]Instituto de Ciencias, Facultad de Medicina, Clínica Alemana Universidad del Desarrollo, Santiago 7710162, Chile

Supporting Information

ABSTRACT: We herein report on the usefulness of the reactivity indices profiles along a reaction coordinate. The model is tested to fully describe the reaction mechanism of the title reactions. Group nucleophilicity and electrophilicity profiles help describe the bond-breaking/bond-formation processes and the intramolecular electron density reorganization. The reactivity indices' profile analysis is consistently complemented with hydrogen bonding (HB) effects along the reaction coordinate: the final outcome of the reaction is determined by the stage at which the HB complex can be formed. Transition-state structures located for six reactions studied, including the charged nucleophile thiocyanate, show that the main stabilizing interaction is that formed between the hydrogen atom of the nucleophile and the *o*-NO_2 group. This result discards the role of HB interaction between the nucleophile and the leaving group previously proposed in the literature.

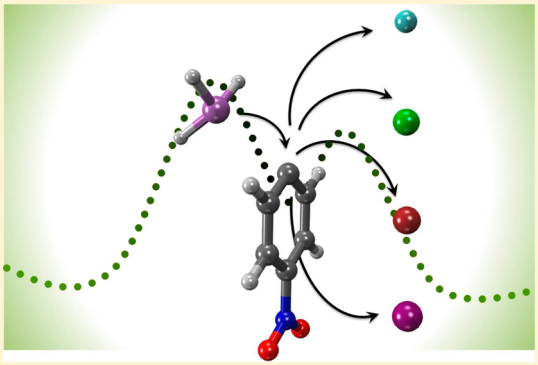

INTRODUCTION

The analysis of the global and regional response functions of the conceptual density functional theory along a well-defined reaction coordinate may become an extremely useful tool to deal with several problems related to the way in which a chemical reaction occurs.[1] For instance, the information embodied in the analysis of reactivity indices along the intrinsic reaction coordinate (IRC) may give important clues about the factors that determine the rate-limiting step, the stability of possible reaction intermediates or transition state (TS) structures, and a semiquantitative ordering of nucleophilicity, electrophilicity, and leaving group abilities (nucleofugality). Profiles of hardness and softness and electronic chemical potential have been proposed to study internal rotations of molecules and simple proton-transfer processes.[2−7]

In this study, we illustrate how the fugality and philicity indices profiles can assist the analysis of a reaction mechanism. The model reaction used is the nucleophilic aromatic substitution of 1-X-2,4-dinitrobenzenes (XDNB, X = F, Cl, Br, I) toward morpholine.[8,9] Scheme 1 summarizes the general reaction mechanism.[10]

The generally accepted S_NAr mechanism occurs in activated aromatic compounds bearing good leaving groups (LG). The first step is the nucleophilic attack toward the aromatic ring, leading to the formation of an anionic σ-adduct named Meisenheimer complex (MC). In a second step, the leaving group detaches after an intramolecular proton transfer from the nucleophile to the LG. This last step may or may not proceed via a catalyzed pathway promoted by a second nucleophile molecule.[10]

The S_NAr reaction has been previously analyzed by Um et al.[8,11] These authors proposed a linear relationship between Pauling's electronegativity of the isolated halides X = F, Cl, Br, and I with the rate coefficient k_1 in Scheme 1 for the reaction of XDNB toward secondary alicyclic amines in MeCN and water. The k_1 coefficient only yields information about the first step of the reaction. Because in this type of reactions the leaving group departure takes place after the MC formation, the k_1 coefficient does not contain information about its nucleofugality. Many years earlier, Parker found the opposite relationship for the reaction of XDNB toward thiocyanate in DMF.[12,13] Figure 1 shows a comparison between those results.

Our working hypothesis establishes that the answer to the different behavior observed for the same family may not be in the isolated halide but in the halides in their valence state; that is, the correct answer can be assessed by following their properties (including electronegativity and the related properties) along the reaction coordinate.

The expressions for the reactivity indices pertinent for this study, which include the global nucleophilicity[14] (ω^-) and its regional (group) counterpart (ω_G^-) as well as the global electrophilicity[15] (ω^+) and its regional (group) counterpart (ω_G^+) indices, are defined as follows:

Received: November 15, 2012
Published: January 4, 2013

Scheme 1. General S_NAr Reaction Mechanism

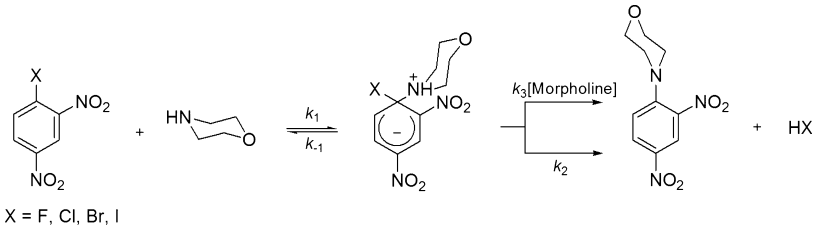

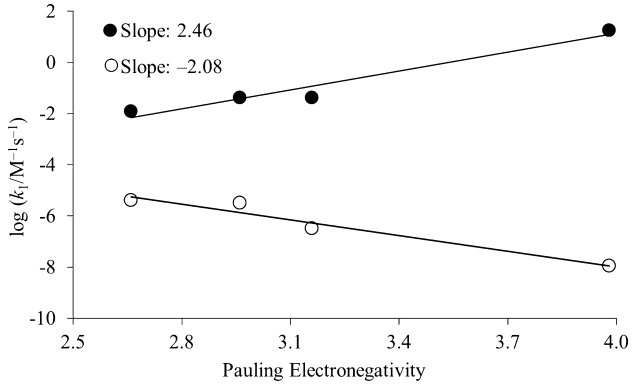

Figure 1. Plots of log k_1 vs electronegativity for reaction of XDNB toward morpholine (filled circles, taken from ref 8) and thiocyanate (empty circles, taken from ref 11). The log k_1 value for the reaction between FDNB and thiocyanate was extrapolated from the published results in ref 11.

$$\omega_G^- = \sum_{k\in G} f_k^- \omega^-;\ \omega^- = \varepsilon_{HOMO} \quad (1)$$

$$\omega_G^+ = \sum_{k\in G} f_k^+ \omega^+;\ \omega^+ = \frac{\mu^2}{2\eta} \quad (2)$$

They are expressed in terms of the electronic chemical potential (μ, the negative of electronegativity) and the chemical hardness (η). The regional (or group) quantities are projected by using the appropriate electrophilic or nucleophilic Fukui functions f_k^+ and f_k^-, respectively, using a method described elsewhere.[16,17] The electronic chemical potential and the chemical hardness were obtained using the frontier molecular orbital HOMO and LUMO.[18]

Before proceeding with the analysis of the reactivity indices, we must define the different molecular regions describing the nucleophile (N), the permanent group (PG), and the leaving group (LG) using an arbitrary fragmentation scheme.[19] The partitioned model is shown in Scheme 2.

RESULTS AND DISCUSSION

Figure 2 displays the TS structures calculated for the six reactions under study.

From the geometric parameters in Figure 2, it is possible to note that the distance between the acidic center in the amine and the LG is large and the hydrogen bond that could be formed will be weak. The distance measured in the hydrogen bond with the *o*-NO_2 group at the TS is within the range of 2.03 Å for X = F to 2.11 Å for X = I. On the other hand, the hydrogen bond with the LG group is larger and is between 2.45 Å and 3.01 Å when X = F and X = I, respectively. In the case of propylamine, the situation is similar, and the hydrogen bond to the *o*-NO_2 is 2.10 Å and with the LG is 2.49 Å. At the other

Scheme 2. General Fragmentation Model of the Electrophile−Nucleophile Pair[a]

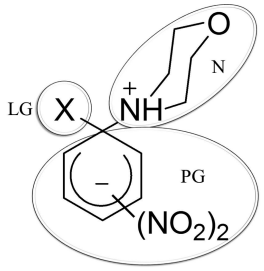

[a]LG, PG, and N stand for leaving group, permanent group, and nucleophile, respectively.

stationary points, namely the R and MC stages, the situation is similar, reinforcing that the main interaction is that formed with the *o*-NO_2 group. Note that for the case of thiocyanate as nucleophile (last structure in Figure 2) the TS structure shows the weakest electrophile/nucleophile interactions.

Figure 3 shows the group electrophilicity profiles for each reaction considered. The analysis is performed within the region including the transition state associated with the nucleophilic attack and the MC formation.

Note that, as expected, the electrophilicity at the N moiety (Figure 3a) is consistently predicted as marginal for the whole series of X = F, Cl, Br, and I. Figure 3b displays the group electrophilicity at the LG moiety. The main result is the sudden enhancement of the electrophilicity of iodine derivative. This result implies that iodine may detach as LG at an early stage of the reaction (prior to the intramolecular proton transfer, see Scheme 1), in agreement with the proposal made by Um et al.[8] Figure 3c illustrates the role of the PG as an electron acceptor fragment within the superstructure shown in Scheme 2. Note that at the MC region the PG becomes electronically saturated. At this point, the intramolecular charge transfer has finished, with the only exception being iodine, which as shown in Figure 3b has begun to detach from the structure in the form of iodide. In summary, the group electrophilicity profile encompasses the entire collection of information about bond formation/bond breaking processes.

Figure 4 shows the profiles associated with the group nucleophilicity of the three fragments defined in Scheme 2.

Figure 4a displays the group nucleophilicity centered at the morpholine moiety. It may be seen that this property dramatically diminishes toward the MC formation for the whole series. The charge transferred from the nucleophile reaches its minimum after the nucleophilic attack. Note that the nucleophilicity centered on the LG and PG fragments (parts b and c, respectively, of Figure 4) reach a maximum value, a result suggesting that the charge is accepted by the PG moiety and redirected to the LG moiety. Even though in all cases the

dx.doi.org/10.1021/jo3025048 | J. Org. Chem. 2013, 78, 1091−1097

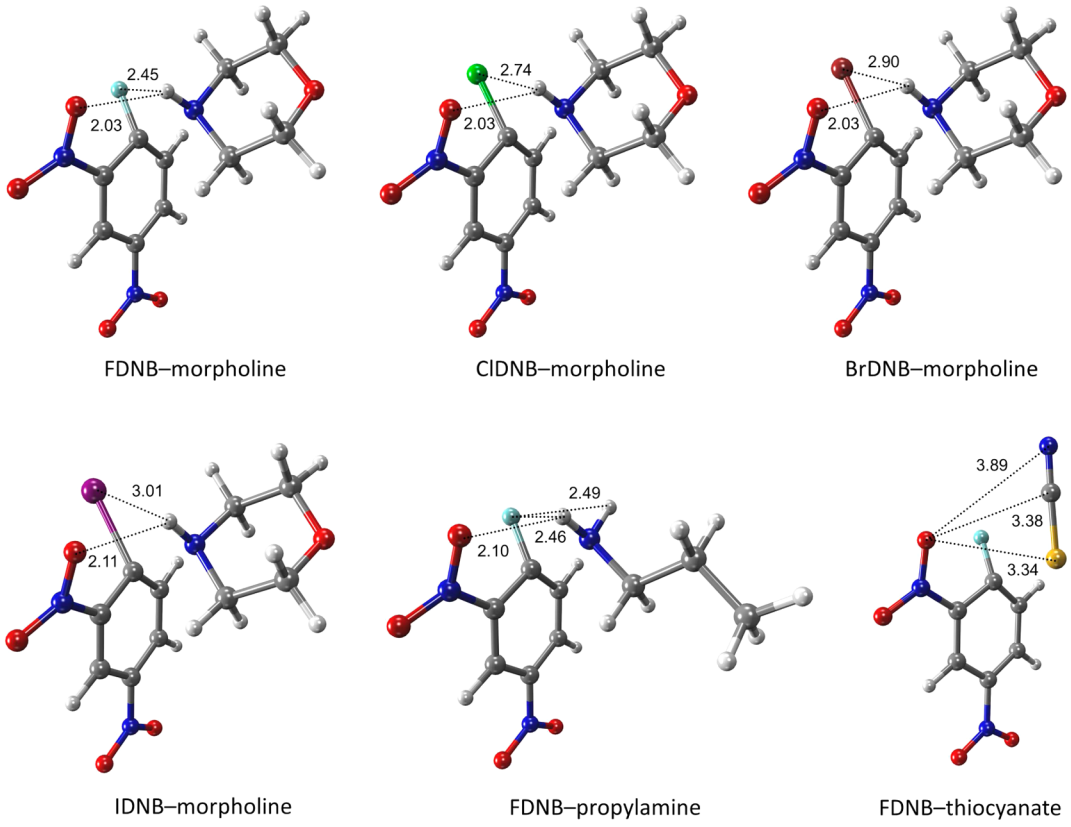

Figure 2. Transition-state structures calculated at the M05-2x/6-31+G(d) level of theory. Distances are in angstroms.

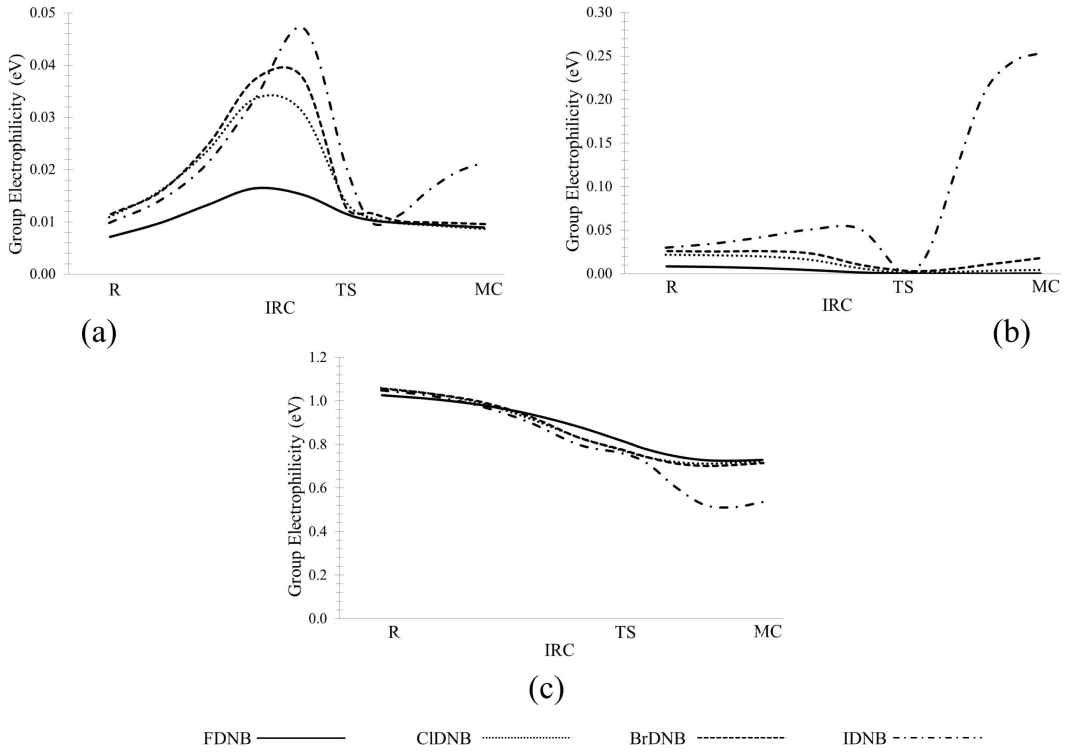

Figure 3. Profiles of group electrophilicity of the fragments centered in the moieties corresponding to: (a) nucleophile, (b) leaving group, and (c) permanent group for the reaction between morpholine toward the XDNB series (X = F, Cl, Br, and I).

nucleophile is the same (morpholine), it is important to stress that the maximum values of the group nucleophilicity of the N moiety are different: 7.29, 6.91, 6.56, and 6.11 eV for X = F, Cl, Br, and I, respectively. This result is relevant because it shows that each substrate interacts in a different way with respect to the nucleophile, and depending on the LG moiety the aromatic

dx.doi.org/10.1021/jo3025048 | J. Org. Chem. 2013, 78, 1091−1097

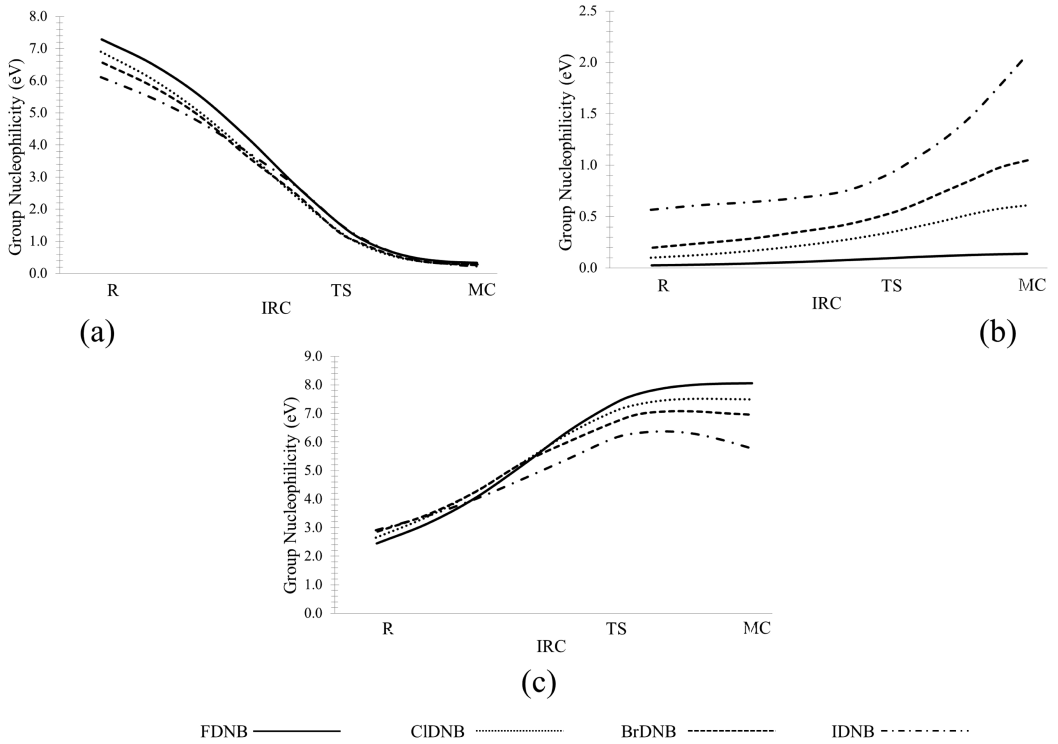

Figure 4. Group nucleophilicity profiles centered in the (a) nucleophile, (b) leaving group, and (c) permanent group for the reaction between morpholine toward 1-X-2,4-dinitrobenzene series (X = F, Cl, Br, I).

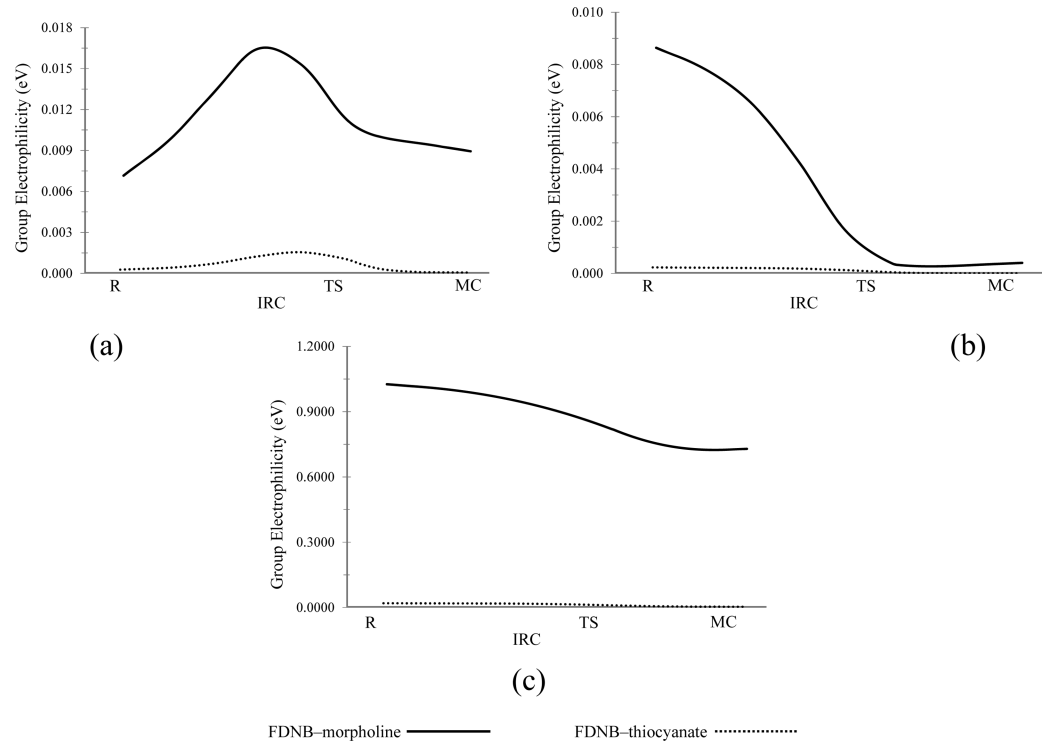

Figure 5. Group electrophility profiles centered in the (a) nucleophile, (b) leaving group, and (c) permanent group for the reaction between morpholine and thiocyanate toward FDNB.

ring may receive a different amount of charge. In Figure 4a, the nucleophilic group donates electronic charge, which is accepted and stabilized at the PG (Figure 4c) and after the TS stage of the reaction redirects this electronic charge toward the LG (Figure 4b). Furthermore, for IDNB, after the TS stage, the PG diminishes its group nucleophilicity by ca. 1.0 eV, thereby indicating that some electronic charge may be further transferred toward the LG. The confirmation of this intramolecular charge transfer is illustrated by the fact that this moiety enhances its nucleophilicity in about the same quantity

dx.doi.org/10.1021/jo3025048 | J. Org. Chem. 2013, 78, 1091−1097

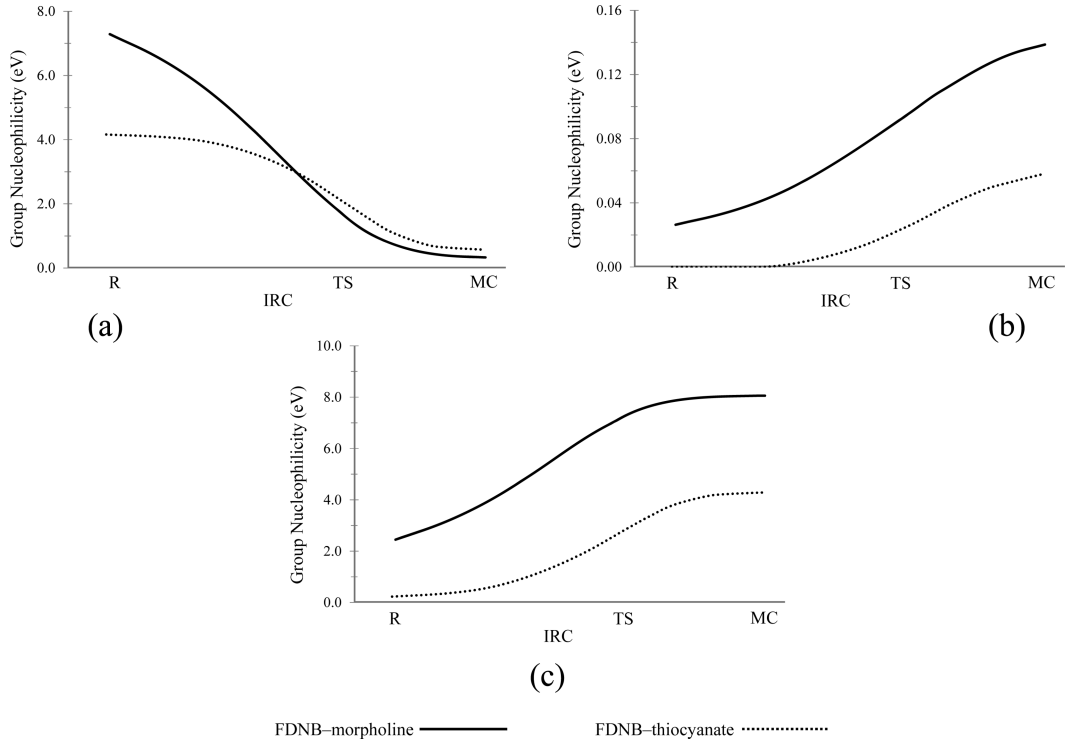

Figure 6. Group nucleophilicity profiles centered in the (a) nucleophile, (b) leaving group, and (c) permanent group for the reaction between morpholine and thiocyanate toward FDNB.

(see Figure 4b). A similar description is observed for LG other than iodine. For instance, for FDNB the PG reaches a maximum without diminishing its group nucleophilicity: Figure 4b shows that for this derivative the LG moiety remains constant along the pathway. In summary, group nucleophilicity profiles also add useful information about intramolecular charge transfer, a process that cannot be quantitatively described by experimental methods.

The effect of intermolecular hydrogen bonding (HB) on the reaction mechanism adds complementary information about the nucleofugality patterns observed for these systems. The electronic analysis may be compared with the experimental results reported by Parker et al. for S_NAr reactions of the same substrates with anionic nucleophiles.[12,13] Therefore, the following LG ability ordering was proposed: I > Br > Cl. In Parker's systems there is not the possibility of such HB interactions because of the nature of the nucleophiles, although the electronic analysis performed above still applies. Following a suggestion by a reviewer, we performed an additional reactivity indices profile analysis for the reaction of FDNB toward thiocyanate and compared these results against the reaction of morpholine with the same substrate. Figures 5 and 6 summarize the result of the electrophilicity and nucleophilicity profiles, respectively. It may be seen that the electrophilicity of the morpholine system is clearly more enhanced as compared to thiocyanate. In the PG (Figure 5c), the activating effect of thiocyanate is marginal. Overall, this comparison highlight that for morpholine as nucleophile, the charge transfer effect toward the substrate FDNB is clearly higher than having thiocyanate as nucleophile. This effect has also consequence on the intramolecular HB formation at the TS. This result is completely in line with the electrophilicity ordering proposed by Parker[13] and Um.[8]

Figure 6 displays the group nucleophilicity profiles for the reaction of morpholine and thiocyanate toward FDNB. It may be seen that morpholine becomes more nucleophilically activated than thiocyanate (Figure 6a). Figure 6b reveals that, as shown previously, the LG moiety has not a significant effect on the nucleophilic attack step of the reaction. The analysis of Figure 6a,c suggests that the nucleophile/electrophile interaction induced by an intramolecular HB formation activates both the nucleophile and the substrate. This comparison reinforces again the hypothesis that intramolecular HB formation at the TS facilitates the nucleophilic attack.

Following the proposal of Um et al., the reaction pathway can be modified by the nature of the nucleophile[8] or by solvent effects.[11] In systems where HB interactions are feasible, the LG is the complex H–X, not X^-. The final situation will be determined by the stage of the reaction at which the HB complex can be formed. It is then clear from Figure 4b that the IDNB substrate may release its LG before the proton-transfer step because the iodide anion is a good leaving group. Because of the stability of iodide and bromide, the proton transfer from the amine attached to the PG to the LG can be predicted as a very slow process. On the other hand, fluoride and chloride are less stable than the former and therefore the release from the MC is expected to be a slow process which may be assisted by proton transfer from the amine. This result definitively explains the apparent contradictory outcomes reported by Um[8] and Parker[13] and condensed in Figure 1. For instance, when the nucleophiles have acidic protons the nucleofugality trend is expected to change to: *F* > Cl > Br > I.

Additional useful information that can complement the reactivity indices profiles may be obtained from natural bond orbital analysis (NBO),[20,21] including HB effects. It is well-known that the main interaction in S_NAr reactions is that formed between the *o*-NO_2 fragment in the PG and the proton

dx.doi.org/10.1021/jo3025048 | J. Org. Chem. 2013, 78, 1091–1097

in the nucleophile.[9,22−24] Second-order perturbation theory analysis is a tool that permits understanding of the interaction from a localized nonbonding orbital (NBO) of an idealized Lewis structure with an empty non-Lewis orbital (see Table 1).

Table 1. Second-Order Perturbation Analysis Performed for the XDNB Substrates in the Reaction with Morpholine at Reactants, Transition State, and the Meisenheimer Complex Intermediate[a]

X	nucleophile	reactants	transition state	MC intermediate
F	morpholine	2.9 (2.33)	10.4 (2.03)	22.7 (1.84)
Cl	morpholine	2.9 (2.31)	10.5 (2.03)	21.1 (1.86)
Br	morpholine	2.5 (2.35)	10.5 (2.03)	18.7 (1.88)
I	morpholine	1.8 (2.41)	6.7 (2.11)	13.7 (1.96)
F	thiocyanate[b]			

[a]The interaction presented is that formed between the antibonding N−H orbital in the nucleophile and the lone pairs in the oxygen atom at the *o*-NO_2 group. All values are expressed in kcal/mol. The hydrogen bond lengths for the same interaction expressed in Å are shown in parentheses. [b]This system does not display any significant nucleophile/electrophile interaction.

For each donor and acceptor orbital i and j, for example, the energy of stabilization is denoted by E_2 and is evaluated as

$$E_2 = \Delta E_{ij} = q_i \frac{F(i,j)^2}{\varepsilon_j - \varepsilon_i} \quad (3)$$

where q_i is the donor orbital occupancy, ε_i and ε_j are diagonal elements, and $F(i,j)$ is the off-diagonal element of the Fock matrix.

The second-order perturbation theory analysis summarized in Table 1 shows the energy values for the antibonding N−H orbital in the nucleophile and the lone pairs in the oxygen atom at the *o*-NO_2 group. This interaction in the whole series of substrates at the reactants stage shows similar and lower values than for the other stationary points in the energy profiles. This result is natural because at this stage of the reaction the species involved are very far away. However, at the transition state the values are similar for X = F, Cl, and Br and lower for X = I. These results illustrate the stabilizing role of the hydrogen bond, which is in agreement with the kinetic data reported by Um et al.[8] The marginal interaction in IDNB is interpreted as a lower stabilizing attraction and consequently a slower reaction. Finally, at the Meisenheimer complex stage this interaction is different and depends upon the LG present in each substrate. For X = F, E_2 = 22.7 kcal/mol and diminishes toward X = I for which E_2 = 13.7 kcal/mol. These results are interpreted here on the basis of the net stabilizing effect of the hydrogen bond. Furthermore, the NBO analysis reinforces the analysis obtained by the reactivity indices profiles: together with the results from Figure 3, the MC complex formed for X = I is unstable, and this result suggests again that iodide may leave the system before the proton transfer is completed. The stabilization of the system is achieved by an electrostatic interaction between the anion I^- and the amine/permanent group fragment (the electrofuge). On the other hand, when X = F, the Meisenheimer complex is totally formed and the driving stabilizing interaction is that promoted by hydrogen bond formation as expected from Figure 2 and geometric parameters in Tables 1 and 2.

A final item is worth mentioning. Second-order perturbation analysis was performed considering the possibility of hydrogen bonding between the acidic hydrogen atom in the nucleophile and the LG. This possibility was considered on the basis of the proposed catalytic scheme suggested by Um et al.[8] The results obtained are summarized in Table 2. In order to make reliable comparisons, we considered a primary amine (propylamine) as nucleophile. This amine has two acidic hydrogen atoms in the nucleophilic center and could form a dual hydrogen bond: one with the *o*-NO_2 group and the other one with the LG.

Table 2. Second-Order Perturbation Analysis Performed for the XDNB Substrates in the Reaction with Morpholine and Propylamine at Reactants, Transition State, and the Meisenheimer Complex Intermediate[a]

LG	nucleophile	reactants	transition state	MC intermediate
F	morpholine	<0.1 (2.75)	<0.1 (2.45)	<0.1 (2.38)
Cl	morpholine	<0.1 (2.96)	<0.1 (2.74)	<0.1 (2.69)
Br	morpholine	<0.5 (3.04)	<0.5 (2.90)	0.6 (2.77)
I	morpholine	<0.5 (3.23)	<0.5 (3.01)	0.7 (2.96)
F	propylamine	<0.1 (2.88)	<0.1 (2.46)	<0.1 (2.37)
F	thiocyanate[b]			

[a]The interaction presented is that formed between the antibonding N−H orbital in the nucleophile and the lone pairs at the leaving group. All values are expressed in kcal/mol. The hydrogen bond lengths for the same interaction expressed in Å are shown in parentheses. [b]This system does not display any significant nucleophile/electrophile interaction.

The results in Table 2 are relevant because they show that the main stabilizing interaction is that formed with the *o*-NO_2 group along the reaction coordinate. Note that all values shown in Table 2 are marginal, which demonstrates that the interaction proposed by Um et al. may be not one of the main factors on which the reaction mechanism depends. The result that the main stabilization of the transition state is provided by the *o*-NO_2 group and not by hydrogen bonding with the leaving group are stressed by the HB distances at the stationary points along the IRC in Tables 1 and 2. Note that for the case of thiocyanate the second-order perturbation analysis consistently predicts that this nucleophile will have negligible orbital interaction, thereby producing a marginal electrophilic activation of FDNB moiety at the TS.

■ CONCLUSIONS

We have illustrated the reliability and usefulness of the reactivity indices profiles along a reaction coordinate. Group nucleophilicity and electrophilicity profiles help in describing the bond-breaking/bond-formation processes. Specifically, the group electrophilicity profile correctly discriminates the different nucleofugality of iodine as compared to F, Cl, and Br derivatives: iodine may detach as LG at an early stage of the reaction. The group nucleophilicity centered on the LG and PG fragments describes the electron density reorganization: the charge is accepted by the PG moiety and redirected to the LG moiety. This result is relevant for it shows that each substrate interacts in a different way respect to the nucleophile, and depending on the LG moiety the aromatic ring may receive a different amount of charge. The reactivity indices profile analysis is consistently complemented with hydrogen bonding effects: the reaction pathway will be determined by the stage of the reaction at which the HB complex can be formed. Finally, NBO analysis reinforces the results obtained from the reactivity indices profiles. The MC complex formed for X = I is unstable, and this result suggests again that iodide may leave the system

dx.doi.org/10.1021/jo3025048 | J. Org. Chem. 2013, 78, 1091−1097

before the proton transfer is completed. Transition states located for the six reactions studied, including thiocyanate as nucleophile suggest that the main stabilizing interaction is that formed with the *o*-NO_2 group along the reaction coordinate. The nucleophile thiocyanate appears as a limiting case where the electrophile/nucleophile interactions are marginal. This result discards the role of HB interaction with the leaving group as it was previously reported in literature.

EXPERIMENTAL SECTION

Computational Details. All of the transition-state structures were fully optimized at the M05-2x/6-31+G(d) level of theory.[25] After the optimization procedure, frequency calculations were performed in order to verify the presence of only one anomalous vibration associated to the bond-forming/bond-breaking process. With this information, an IRC calculation was performed to obtain the reaction profile that smoothly connects reactants and the MC intermediate. Finally, the Fukui function[16,17] and NBO analysis[20,21] were performed on selected points along the IRC using a method described elsewhere. All of the calculations were performed using the Gaussian 03 suite of programs.[26]

ASSOCIATED CONTENT

Supporting Information

Cartesian coordinates, energy, and harmonic analysis for all transition-state structures. This material is available free of charge via the Internet at http://pubs.acs.org.

AUTHOR INFORMATION

Corresponding Author

*Tel: (+56 2) 29787272. Fax: (+56 2) 2713888. E-mail: rormazabalt@u.uchile.cl.

Notes

The authors declare no competing financial interest.

ACKNOWLEDGMENTS

This work was supported by Project ICM-P10-003-F, CILIS, granted by Fondo de Innovación para la Competitividad, del Ministerio de Economía, Fomento y Turismo, Chile, and FONDECYT projects 1100492 and 1110062. R.O-T. thanks CONICYT for a doctoral fellowship.

REFERENCES

(1) Miño, G.; Contreras, R. *J. Phys. Chem. A* **2009**, *113*, 5769.
(2) Chandra, A. K.; Uchimaru, T. *J. Phys. Chem. A* **2001**, *105*, 3578.
(3) Chamorro, E.; Chattaraj, P. K.; Fuentealba, P. *J. Phys. Chem. A* **2003**, *107*, 7068.
(4) Elango, M.; Parthasarathi, R.; Subramanian, V.; Sarkar, U.; Chattaraj, P. K. *THEOCHEM* **2005**, *723*, 43.
(5) Jaque, P.; Toro-Labbé, A. *J. Phys. Chem. A* **2000**, *104*, 995.
(6) Kar, T.; Scheiner, S. *J. Phys. Chem.* **1995**, *99*, 8121.
(7) Kar, T.; Scheiner, S.; Sannigrahi, A. B. *J. Phys. Chem. A* **1998**, *102*, 5967.
(8) Um, I. H.; Im, L. R.; Kang, J. S.; Bursey, S. S.; Dust, J. M. *J. Org. Chem.* **2012**, *77*, 9738.
(9) Senger, N. A.; Bo, B.; Cheng, Q.; Keeffe, J. R.; Gronert, S.; Wu, W. *J. Org. Chem.* **2012**, *77*, 9535.
(10) Banjoko, O.; Babatunde, I. A. *Tetrahedron* **2004**, *60*, 4645.
(11) Um, I. H.; Min, S. W.; Dust, J. M. *J. Org. Chem.* **2007**, *72*, 8797.
(12) Cox, B. G.; Parker, A. J. *J. Am. Chem. Soc.* **1973**, *95*, 408.
(13) Parker, A. J. *Chem. Rev.* **1969**, *69*, 1.
(14) Contreras, R.; Andres, J.; Safont, V. S.; Campodonico, P.; Santos, J. G. *J. Phys. Chem. A* **2003**, *107*, 5588.
(15) Parr, R. G.; Szentpály, L. V.; Liu, S. *J. Am. Chem. Soc.* **1999**, *121*, 1922.
(16) Contreras, R. R.; Fuentealba, P.; Galván, M.; Pérez, P. *Chem. Phys. Lett.* **1999**, *304*, 405.
(17) Fuentealba, P.; Pérez, P.; Contreras, R. *J. Chem. Phys.* **2000**, *113*, 2544.
(18) Koopmans, T. *Physica* **1934**, *1*, 104.
(19) Ormazábal-Toledo, R.; Campodónico, P. R.; Contreras, R. *Org. Lett.* **2011**, *13*, 822.
(20) Glendening, E. D.; Reed, A. E.; Carpenter, J. E.; Weinhold, F. NBO Version 3.1.
(21) Reed, A. E.; Curtiss, L. A.; Weinhold, F. *Chem. Rev.* **1988**, *88*, 899.
(22) Bunnett, J. F.; Morath, R. J. *J. Am. Chem. Soc.* **1955**, *77*, 5051.
(23) Bunnett, J. F.; Morath, R. J.; Okamoto, T. *J. Am. Chem. Soc.* **1955**, *77*, 5055.
(24) Chéron, N.; El Kaïm, L.; Grimaud, L.; Fleurat-Lessard, P. *Chem.—Eur. J.* **2011**, *17*, 14929.
(25) Zhao, Y.; Schultz, N. E.; Truhlar, D. G. *J. Chem. Phys.* **2005**, *123*, 1.
(26) Frisch, M. J.; Trucks, G. W.; Schlegel, H. B.; Scuseria, G. E.; Robb, M. A.; Cheeseman, J. R.; Montgomery, J. A., Jr.; Vreven, T.; Kudin, K. N.; Burant, J. C.; Millam, J. M.; Iyengar, S. S.; Tomasi, J.; Barone, V.; Mennucci, B.; Cossi, M.; Scalmani, G.; Rega, N.; Petersson, G. A.; Nakatsuji, H.; Hada, M.; Ehara, M.; Toyota, K.; Fukuda, R.; Hasegawa, J.; Ishida, M.; Nakajima, T.; Honda, Y.; Kitao, O.; Nakai, H.; Klene, M.; Li, X.; Knox, J. E.; Hratchian, H. P.; Cross, J. B.; Bakken, V.; Adamo, C.; Jaramillo, J.; Gomperts, R.; Stratmann, R. E.; Yazyev, O.; Austin, A. J.; Cammi, R.; Pomelli, C.; Ochterski, J. W.; Ayala, P. Y.; Morokuma, K.; Voth, G. A.; Salvador, P.; Dannenberg, J. J.; Zakrzewski, V. G.; Dapprich, S.; Daniels, A. D.; Strain, M. C.; Farkas, O.; Malick, D. K.; Rabuck, A. D.; Raghavachari, K.; Foresman, J. B.; Ortiz, J. V.; Cui, Q.; Baboul, A. G.; Clifford, S.; Cioslowski, J.; Stefanov, B. B.; Liu, G.; Liashenko, A.; Piskorz, P.; Komaromi, I.; Martin, R. L.; Fox, D. J.; Keith, T.; Laham, A.; Peng, C. Y.; Nanayakkara, A.; Challacombe, M.; Gill, P. M. W.; Johnson, B.; Chen, W.; Wong, M. W.; Gonzalez, C.; Pople, J. A. *Gaussian 03, Rev. E.01*, Gaussian, Inc., Wallingford, CT, 2004.